

THE LASER REFERENCE LINE METHOD AND ITS COMPARISON TO A TOTAL STATION IN AN ATLAS-LIKE CONFIGURATION

V. Batusov^a, *J. Budagov*^a, *M. Lyablin*^a,
J.-Ch. Gayde^b, *B. Di Girolamo*^b, *D. Mergelkuhl*^b, *M. Nessi*^b

^a Joint Institute for Nuclear Research, Dubna

^b CERN, Geneva

A new type of measuring system, the Laser Reference Line (LRL), is proposed as a metrological tool and can be used within limited space to ensure a precise installation along an axis on the ATLAS interaction point. A simplified ATLAS-like beam-pipe mock-up is used for this test. The coordinates of the beam pipe are measured three times using the new method and a Total Station. The measurements agree within the measurement error of the Total Station, which indicates that the precision of the laser reference line is suitable for this specific task in the ATLAS experiment.

В качестве метрологического инструмента предлагается новый тип измерительной системы — лазерная реперная линия. Она может использоваться в условиях ограниченного пространства для обеспечения высокоточной установки оборудования спектрометра ATLAS относительно оси в месте столкновения пучков. В качестве теста использовался имитационный макет пучковой трубки. Измерения координат концов трубки проводились при помощи лазерной реперной линии и тахеометрической измерительной системы. Результаты согласуются в пределах погрешности измерений тахеометра, показывая, что точность лазерной реперной линии адекватна конкретной задаче в эксперименте ATLAS.

PACS: 06.60.Sx

INTRODUCTION

A number of metrological demands concern highly precise installation of experimental equipment under the conditions of reduced space for installation of generally employed geodetic tools and a free line-of-sight to the measured equipment. This applies to the Total Station [6] that is intended to be used for precise installation of the beam pipe inside the ATLAS detector. An alternative solution for this kind of demand could be the Laser Reference Line (LRL) measuring system with the laser beam that serves as the reference axis with respect to which one can determine and also set equipment to a desired position in accordance with the measured data and carry out on-line monitoring [1–5].

To confirm experimentally the possibilities of laser-based techniques in precise mounting of equipment, the coordinates of the pipe ends have been measured using the Total Station

and, at the same time, the laser reference line in a simple mock-up of the ATLAS experiment at CERN. The results of the measurements indicate that laser-based techniques can in principle be used for metrological measurements and the system is at the level of precision asked for the beam pipe installation in the ATLAS detector.

The obtained results show that the system is compatible with high-precision metrological measurements and is at the level of precision at the specific circumstances of the ATLAS detector.

1. FORMULATION OF THE ATLAS NEEDS

Upgrading of the ATLAS detector involves replacement of the 6-m beam pipe in its central part. Figure 1 schematically shows the arrangement of the replaceable beam pipe T and the beam pipes BP₁ and BP₂ taken as reference parts in the ATLAS underground experimental hall.

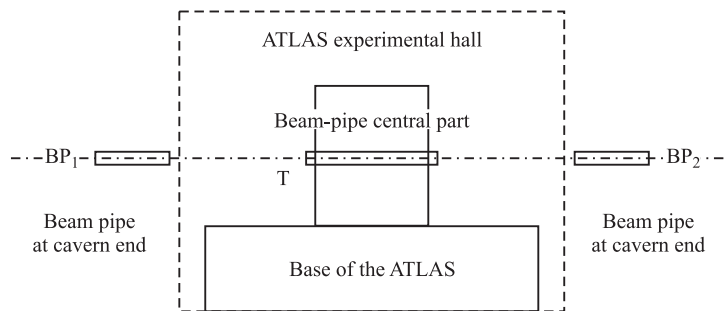


Fig. 1. Location of the central part of the beam pipe in the ATLAS experimental hall

The new beam pipe has to be positioned with accuracy better than 100 μm relative to the BP₁ and BP₂ that are used as reference. Yet, the current accuracy of the so far used Total Station [6] to perform measurements at ATLAS is ± 0.2 mm, and its use is limited by the difficult access to the pipes in question. The link of the local measurements of the LRL system with respect to the global coordinate system of the accelerator needs to be done using a Total Station.

Under these conditions the authors proposed to use the LRL method as a new-generation metrological precision system capable of operating within confined space.

2. LASER REFERENCE LINE: OPERATION AND DESIGN

2.1. General Design. The LRL measuring system uses a laser beam with known positions of the beginning and end points. The laser beam source can be precisely adjusted using the so-called two-axis angular positioner for positioning in the azimuthal θ and polar φ angles and the position-sensitive quadrant photodetector QPr¹ to determine the beam axis position (Fig. 2) [7].

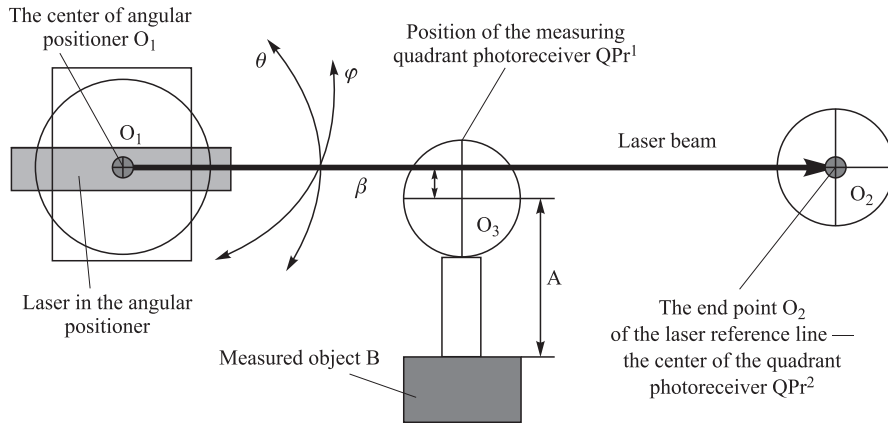


Fig. 2. Diagram of the LRL system

The LRL reference points are the starting point O_1 , which is the center of the angular positioner of the laser beam source (determined by direct measurements with the two-axis angular positioner), and the end point O_2 , which is the center of the end quadrant photodetector QPr^2 .

In numerous metrological demands it is necessary to measure coordinates of an object in the transverse directions with respect to the laser beam. In the case considered in Fig. 2 the position of the measured object B relative to the LRL is defined as a sum of the known distance A (center O_3 of QPr^1 to the object B) and the distance β that is determined with the help of QPr^1 measurements.

2.2. Pipe Adjustment. The procedure for the adjustment of the beam pipe position relative to the laser reference line is illustrated in Fig. 3.

The laser beam source is placed in the support pipe BP_1 and the adapter A_2 with the QPr^2 is aligned in the support pipe BP_2 . The coordinates of the BP_1 and BP_2 pipe ends are simultaneously determined by the Total Station in a global coordinate system X, Y, Z and in

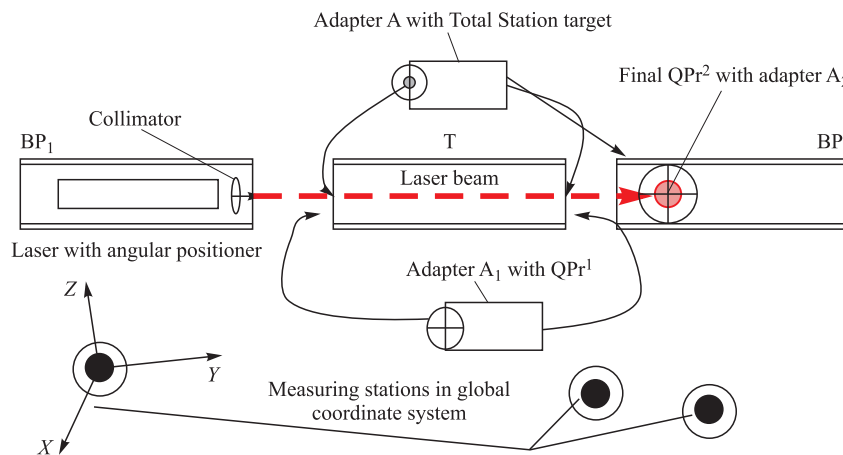


Fig. 3. The LRL measurement system for precise measurement of two transverse coordinates of the beam-pipe mock-up T

the LRL coordinate system. A Total Station target with a special cylindrical adapter with the size of the inner diameter of the support pipes is used. The adapter A with the Total Station target is inserted alternatively in the exit ends of the pipes BP₁ and BP₂, which allows the coordinates of their exit hole centers to be determined by the Total Station. The LRL is thus transformed into the global coordinate system using the Total Station measurements. Further this procedure is used for regularly checking the positions of the LRL reference points.

The adapter A₁ with the photodetector QPr¹ serves to check alignment of the coaxial position of the LRL with respect to the pipes BP₁ and BP₂ and to measure coordinates of the pipe T ends.

Thus, the scheme shown in Fig.3 allows one to include the LRL in a global coordinate system and then to perform measurements and pipe adjustment in it.

2.3. LRL Adjustment of the Pipe. A basic diagram concerning the procedure for the determination of coordinates of central pipe ends can be found in Fig. 4.

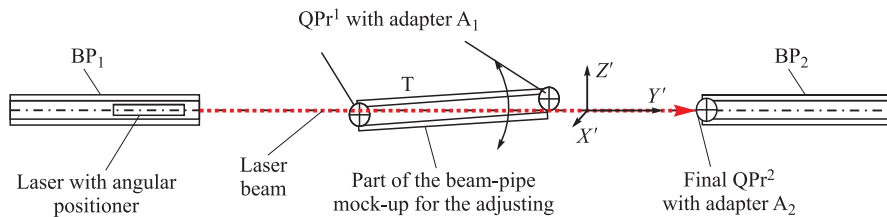


Fig. 4. Measurement of the coordinates of the ends of the beam-pipe mock-up positioned along the LRL

The diagram shows the measurement of the transverse coordinates of the ends of the pipe T in the X', Y', Z' coordinate system of the laser reference line. The beam runs through the pipe T, and the centers of its ends prove to be initially off the LRL axis.

The X', Z' coordinates of the pipe T ends are determined using the QPr¹ with a special cylindrical adapter A₁, which fits precisely the inner diameter of the pipe T. The mechanical precision for the fabrication of the adapters is ± 0.02 mm in diameter. The adapter A₁ is inserted alternatively in the left and the right ends of the pipe T so that the laser beam hits the QPr¹. After the detection of the signals from the quadrant photodetector, the coordinates of the ends of the pipe T are determined relative to the laser beam axis. Thus, the obtained coordinates of the centers of the ends of the pipe are converted from the local laser coordinate system to the global coordinate system.

3. JOINT LRL AND TOTAL STATION MEASUREMENT PROCEDURE

3.1. Basic Scheme. The purpose of the ATLAS mock-up has been to determine the coordinates of the positions of the ends of the pipe T using the Total Station and the laser reference line. The basic measurement diagram for this is shown in Fig. 5.

The laser reference line has been established using the system of reference pipes T₁ and T₂. The Total Station has measured the base positions C and D in the global X, Y, Z coordinate system. First, the coordinates of points A, B₁, B₂, and B have been measured in the global X, Y, Z coordinate system using the adapter A with the Total Station target. Then

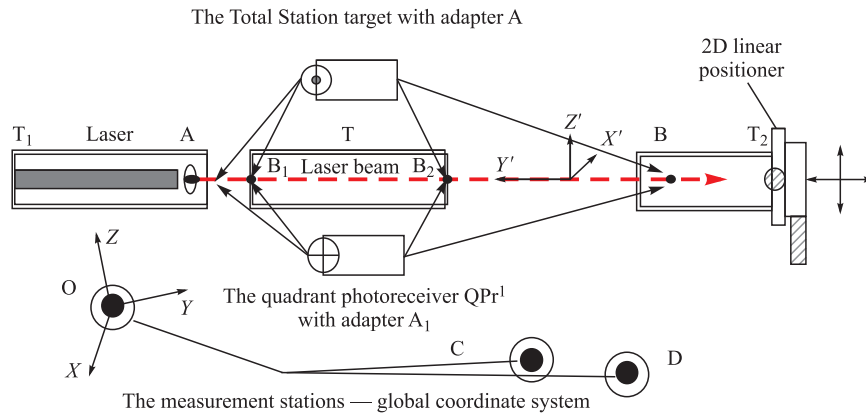


Fig. 5. Diagram of joint measurement of the pipe T end positions B_1 and B_2 by the Total Station and LRL

the coordinates of points B_1 and B_2 were measured in the local coordinate system X', Y', Z' (C'S) using the LRL.

The comparison of the measurement results has been performed in the local coordinate system C'S.

Let us consider in more detail the joint measurement procedure and comparison of the Total Station and LRL measurement results.

3.2. LRL Adjustment. The LRL system parts have been installed in the pipes T_1 and T_2 . A two-axis linear positioner with a precision of $\pm 3 \mu\text{m}$ has been used for positioning the LRL end point, as a high-precision (10^{-6} rad) angular positioner for laser adjustment has not been available by the time of the test experiments. A He-Ne laser has been installed co-axially inside the pipe T_1 using a cylindrical adapter. The He-Ne laser has been roughly adjusted to point the laser beam spot on the center B of the tube T_2 end. The test arrangement has been simplified by using a single quadrant photodetector and a universal adapter, which served to adjust the LRL and to perform joint measurements. To achieve this, the inner diameter of the tubes T_1 , T, and T_2 have been taken to be equal to the outer diameter of the QPr adapter. This allowed the photodetector in the cylindrical adapter to be used to measure the coordinates of all the pipe ends (T_1 , T_2 , T). Once the adapter with the QPr is inserted in the pipe T_2 , the position of the spot of the approximately adjusted laser beam is detected and the pipe T_2 is aligned with the laser beam using the two-axis linear positioner. In doing this, we seek to have equal signals for all the four quadrant photodetectors. After checking the alignment of the laser beam and the pipe T_2 , we finish the LRL adjustment procedure using the QPr.

3.3. Local Coordinate System in the Joint Measurements of the Laser and Total Station Measurement Systems. The reference points A and B of the laser reference line have been measured in the global coordinate system of the Total Station, as is shown in Fig. 5. Similarly, it is possible to create a common local system of coordinates X', Y' , and Z' (Fig. 6) that has been chosen to perform comparative measurements of the Total Station and LRL measuring systems.

The point A, coinciding with the center of the Total Station target at the end of the pipe T_1 , has been defined as origin for the coordinate system. The Y' axis has been directed in the opposite sense of the laser beam direction and run through the center of the Total Station

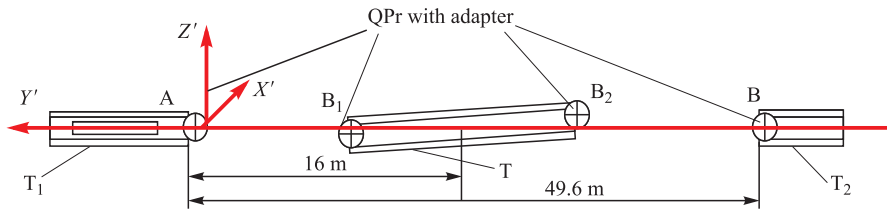


Fig. 6. Definition of a local coordinate system X', Y', Z' for joint measurements of the Total Station and LRL measuring system

target at the end of the pipe T_2 . The laser beam axis coincides with the Y' axis. The Z' axis is in the plane formed by the gravity vector and the Y' axis. The Z' axis is perpendicular to the Y' axis, and the X' axis is perpendicular to the Z' and Y' axes. Comparison has been performed for the transverse coordinate directions Z' and Y' .

3.4. Total Station Measurement Procedure. The centers of the ends of the pipe T called B_1 and B_2 and the LRL reference points A and B have been measured using the adapter A (Fig. 5). The cylindrical adapter for the Total Station target fits precisely in the inner diameter of the pipes T_1 , T, and T_2 . Measurements have been carried out and the new measured points A, B, B_1 , and B_2 have been added in the global coordinate system to the positions of the points C and D. Then the misalignment of the pipe ends B_1 and B_2 and the Y' axis has been determined in the chosen local X', Y', Z' coordinate system.

The reference points A and B of the laser reference line are determined by the Total Station measurement, which further allows measurements in the local X', Y', Z' coordinate system. After that the coordinates of the ends of the pipe T obtained by the two different measurement systems have been compared.

3.5. LRL Measurement Procedure. A single-mode He-Ne laser with a collimator to produce a collimated laser beam over 50 m has been used in the experiment. The LRL length has been 49.6 m, and the distance from the laser to the pipe T has been 16 m (Fig. 6). The pipe T has been approximately aligned with the LRL laser beam. For the mock-up a QPr has been used with a light-sensitive zone of 8 mm in diameter.

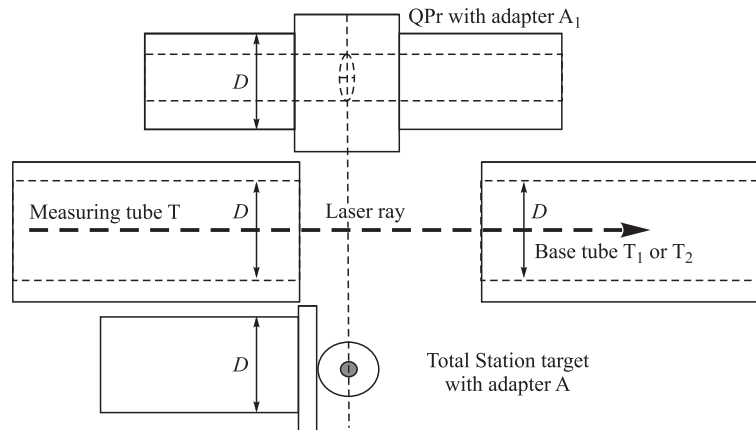


Fig. 7. Positions of the Total Station and photometric adapters at the pipe ends

An adapter with the quadrant photodetector QPr is used to measure the coordinates of the ends of the pipe T relative to the laser beam. Once it has been inserted into the pipe T, signals from four quadrant photodetectors have been measured. The positions of the ends of the pipe T have been determined relative to the laser beam axis in the vertical (Z' axis) and horizontal (X' axis) directions using the measurement data and the calibration curves (see below).

The laser measurements have been performed using a specially designed adapter A_1 for the quadrant photodetector (Fig. 7).

The quadrant photodetector with adapter A_1 has been placed inside the pipe T at both ends so that the surface of the photodetector is perpendicular to the laser beam and its center coincides with the center of the Total Station target with the adapter A. This compensates the systematic error in the transverse X' and Z' coordinates that could be caused by a tilt of the pipe T with respect to the Y' axis during the Total Station and LRL measurements (Fig. 5).

3.6. Laser Measurement Calibration. Calibration measurements have been performed to determine the dependence of the quadrant photodetector signal on the known photodetector displacement, which has been set by the micrometer screw of the positioner.

Four series of calibration measurements have been performed at the distance of the pipe T (16 m) using a two-axis linear positioner with a quadrant photodetector attached to it (Fig. 8).

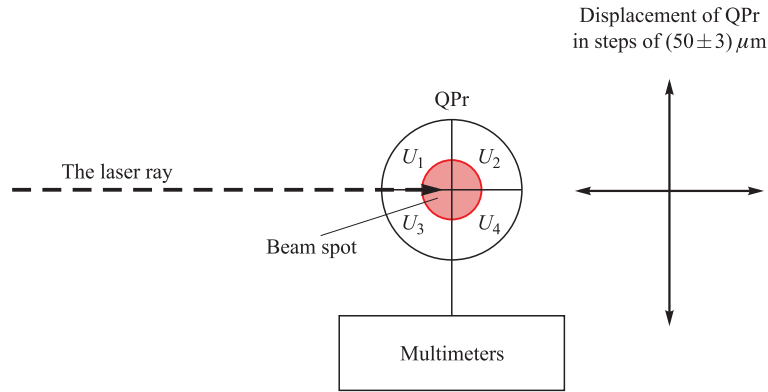


Fig. 8. Diagram of calibration measurements with a single-mode laser beam

Data of the quadrant photodetector QPr have been collected using multimeters with relative accuracy 10^{-4} . The positioner has been moved in steps of $(50 \pm 3) \mu\text{m}$. The movements of the two-axis positioner start from the center of the laser beam. All photodetector readings are expected to be identical in this position by virtue of the symmetric distribution of the laser radiation power over the beam cross section.

The following dimensionless quantities have been used as signals:

$$\begin{aligned} S_{\text{up}} &= \frac{(U_1 + U_2) - (U_3 + U_4)}{U}, & S_{\text{down}} &= \frac{(U_3 + U_4) - (U_1 + U_2)}{U}, \\ S_{\text{left}} &= \frac{(U_2 + U_4) - (U_1 + U_3)}{U}, & S_{\text{right}} &= \frac{(U_1 + U_3) - (U_2 + U_4)}{U}. \end{aligned} \quad (1)$$

Here $U_1, U_2, U_3,$ and U_4 are the signals of the four individual quadrants of the photodetectors and $U = U_1 + U_2 + U_3 + U_4$ is the total signal of the four photodetectors QPr.

The results of the Total Station measurements are presented in the local X', Y', Z' coordinate system; the vertical Z' axis lies in the plane formed by the gravity vector and the Y' axis (see above), and the longitudinal X' axis is horizontal. Therefore, in order to compare the results of both techniques, the laser measurements of $U_1, U_2, U_3,$ and U_4 have been performed with the quadrant photodetector oriented in a way that the photodetector division line AB has been perpendicular to the gravity vector (Fig. 9).

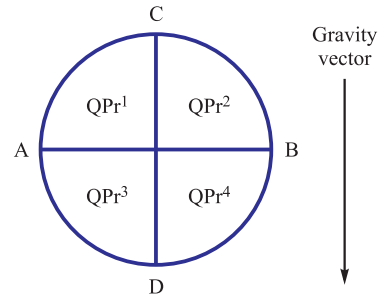


Fig. 9. Position of the quadrant photodetector for horizontally (A, B) and vertically (C, D) performed measurements

The calibration measurements have been performed in four different directions: up, down, left, and right.

3.7. Errors in Calibration Curve Measurements. The quadrant photodetector signals $U_1, U_2, U_3,$ and U_4 have been measured with fluctuations caused by the fact that the beam is propagated in the air. Investigation into the influence of such a fluctuation in [8] shows that at a distance of 16 m the root-mean-square transverse deviation of the laser beam axis is as large as $15 \mu\text{m}$, which introduces an error in the measurement of the laser beam spot position on the quadrant photodetector. To compensate for this in the present conditions, the error δU in the measurement of the photodetector signal has been calculated from several series of photodetector signal measurements with the laser beam axis position «at the QPr center». The errors in the quantities $S_{\text{up}}, S_{\text{down}}, S_{\text{left}},$ and S_{right} , see (1), have been taken into account for the calculation. The major error in determination of the quadrant photodetector displacement during the calibration measurements is the inaccuracy¹ of the QPr positioning in the laser beam axis and for this δU has been taken into account.

3.8. Results of the Measurements. Figures 10 and 11 show the calibration curves S_i ($S_{\text{up}}, S_{\text{down}}, S_{\text{left}}, S_{\text{right}}$) calculated by formulas (1).

Figures 10 and 11 show that the S_i values for the up/down and left/right displacements coincide within the error, which points to the symmetric distribution of the laser beam power in the horizontal and vertical directions. Figure 12 shows the averaged data from Figs. 10 and 11 in vertical and horizontal directions.

It is visible in Fig. 12 that measurements in the horizontal and vertical directions have equal values up to the displacement $\delta \approx 0.5 \text{ mm}$. When $\delta \geq 0.5 \text{ mm}$, a discrepancy arises between the \bar{S}_{hor} and \bar{S}_{vert} values, which can be interpreted as an asymmetry of the laser beam power distribution (Fig. 13).

The difference $D = \bar{S}_{\text{hor}} - \bar{S}_{\text{vert}}$ between the signals in the vertical and horizontal directions has been investigated for values of $\delta \geq 0.5 \text{ mm}$ (Fig. 14) and an average value of $D_{\text{av}} = 0.027$ has been found.

The parameter D_{av} , which corresponds to the average distance between the \bar{S}_{hor} and \bar{S}_{vert} curves in Fig. 13, indicates the difference between the laser beam power distributions in the

¹See Subsec. 3.9 for more detail.

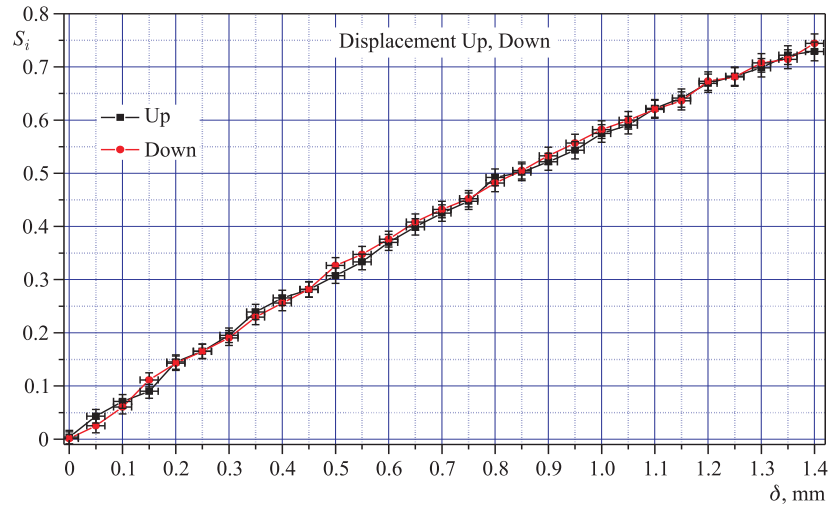


Fig. 10. Calibration measurements: dependence of S_i on the up/down test displacements δ

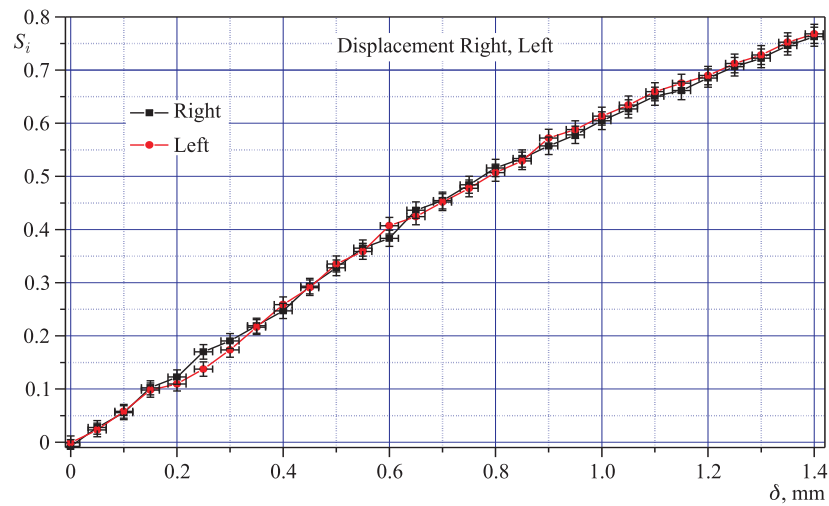


Fig. 11. Calibration measurements: dependence of S_i on the left/right test displacements δ

horizontal and vertical planes. If the approximately equal slope of the curves in Fig. 13 is considered, a displacement $\overline{\Delta\delta}$ corresponding to D_{av} is $\overline{\Delta\delta} = 35 \mu\text{m}$. In fact, this value of $\overline{\Delta\delta}$ determines the asymmetry between a laser beam in the horizontal and vertical directions in the dimensional values.

The difference between the power distributions in the horizontal and vertical cross sections of the laser beam limits the measurement accuracy if an averaged calibration over two directions is used (Fig. 15). Indeed, it is seen in Fig. 15 that the error in the measurements of the transverse laser beam coordinates increases with an increasing displacement δ , and at $\delta \approx 0.5 \text{ mm}$ this error is $\pm 50 \mu\text{m}$, and at $\delta \approx 1.4 \text{ mm}$ it is as large as $\pm 100 \mu\text{m}$.

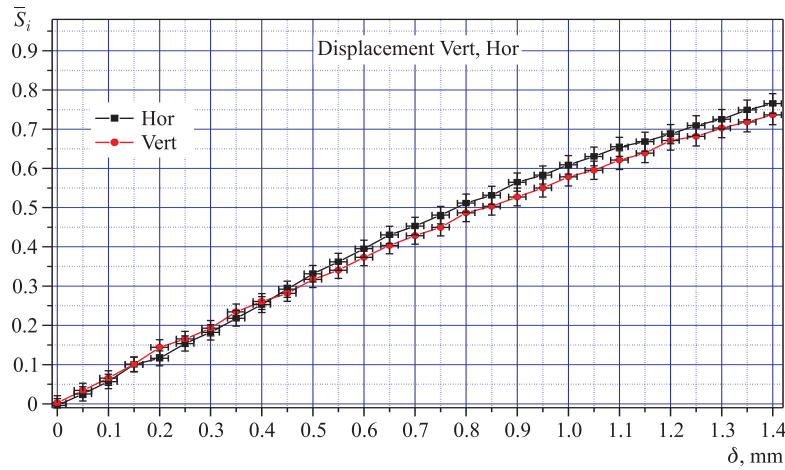


Fig. 12. Calibration measurements: dependence of averaged \bar{S}_i on the horizontal and vertical test displacements δ

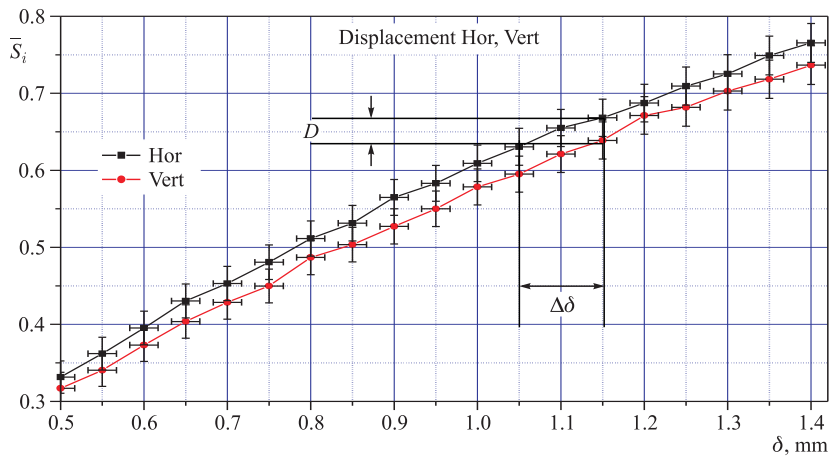


Fig. 13. Dependence of \bar{S}_{hor} and \bar{S}_{vert} on the displacement δ when $\delta \geq 0.5$ mm

It is this calibration that has been used for the coordinate measurement of the centers of the ends of the pipe T (Fig. 5).

The laser measurement data has been transformed to fit the global coordinate system of the Total Station measurements, for the comparison with the Total Station measurement data.

3.9. LRL Measurement Accuracy. The following sources influence the LRL measurement accuracy:

- inaccurate setting of the laser beam reference points with respect to the ends of the reference pipes;
- fluctuation of refractive index of the air in which the laser beam propagates;
- distortion of the laser beam shape by the collimation system;

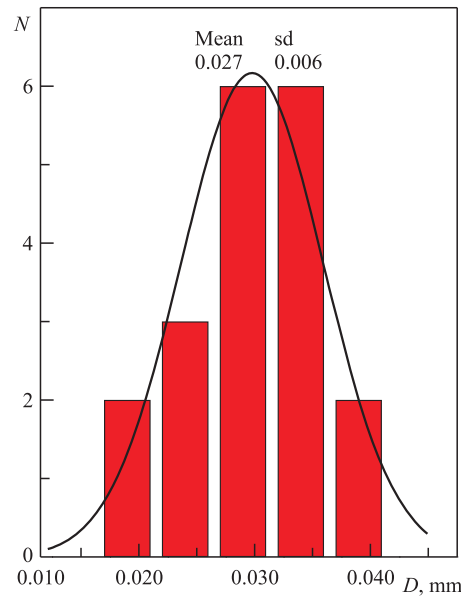


Fig. 14. Distribution of $D = \bar{S}_{hor} - \bar{S}_{vert}$ as obtained from the calibration plots

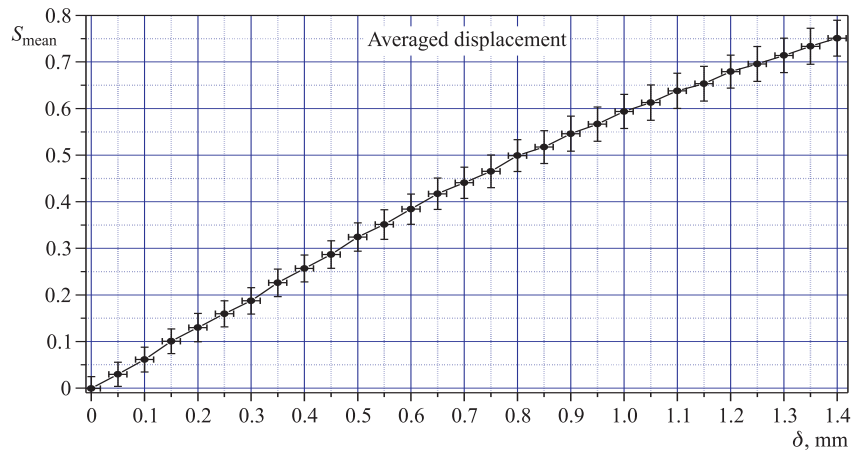


Fig. 15. Averaged calibration values of S_{mean} as a function of δ

- accuracy of the calibration measurement system, which should be taken into account if the local LRL coordinate system is linked to the global coordinate system;
- perpendicularity of the QPr with respect to the laser beam during the measurement.

If two pipes are used as a base for the reference points, the determination accuracy of the reference points — ends of these pipes — depends on the alignment accuracy of the calibration QPr adapter and the positioning accuracy of the quadrant photodetector in the adapter. According to our evaluations, the positioning accuracy of the adapter in the pipe and of the QPr in the adapter can be as high as $\sigma_{pos} = 10 \mu m$.

The fluctuation of the refractive index of the air results in laser beam jitter. Investigations to determine the root-mean-square deviation of the transverse laser beam oscillation σ in the air have been carried out in [8]. They revealed a nonlinear dependence of σ_{fl} on the distance and gave a value of $\sigma_{fl} = 85 \mu\text{m}$ over a length of 50 m.

Distortion of the laser beam shape by the optical collimator introduces an additional measurement error if the laser beam is assumed to be symmetric. As is shown above, this leads to an additional error of $\sigma_{asym} \approx 20 \mu\text{m}$.

Thus, a consideration of all error sources determines the overall LRL measurement error that is presented in Fig. 16.

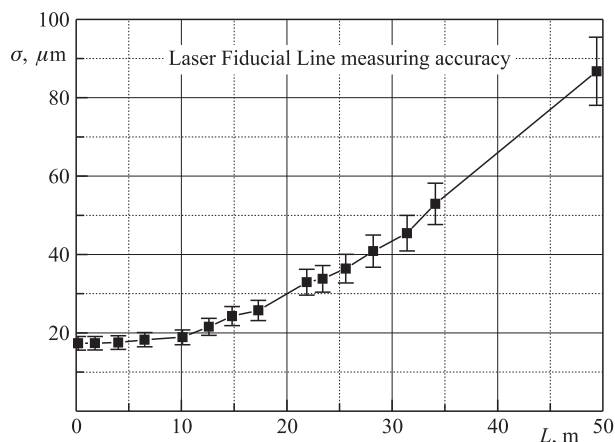


Fig. 16. Measurement error for laser reference line as a function of length L

Precision optics and highly accurately manufactured adapters could increase the LRL measurement accuracy for small distances ($L < 10$ m), but the major source of errors in the LRL measurements will be air fluctuations.

With suppression of the air refractive index fluctuations in a pipe with standing sound waves, see references [8–10], the measurement accuracy will depend mainly on the LRL setting and can be at a level of few micrometers.

3.10. Determination of the Coordinates of the Pipe Ends Using the Averaged Calibration Curve. Signals from the photodetectors are recorded using multimeters once the quadrant photodetector QPr with the adapter A_1 is inserted into the pipe T (Fig. 5).

The scheme in Fig. 17 shows the position of the laser beam spot on the quadrant photodetector.

Since the center of the laser beam spot corresponds to the point of passage of the Y' axis through the end of the pipe T (Fig. 5), we define the 2D coordinate system X', Z' , in which we find the coordinates $d_{X'}$ and $d_{Z'}$ of the quadrant photodetector center B, which corresponds to the measured tube end.

To this end, using the readings of the quadrant photodetectors, we find the values of the function S in the horizontal and vertical directions. Then, using the averaged calibration curve data (Fig. 14), we get the coordinates $d_{X'}$ and $d_{Z'}$ of the quadrant photodetector QPr center.

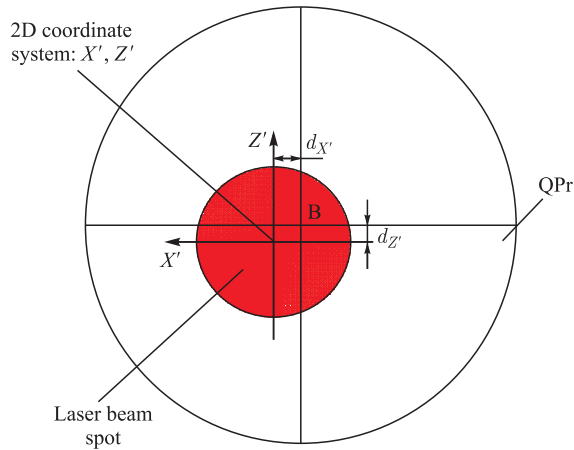


Fig. 17. Determination of the coordinates of the quadrant photodetector center in the 2D coordinate system X', Z'

Further the coordinates $d_{X'}$ and $d_{Z'}$ of the center of the end of the pipe T are compared with the corresponding coordinates obtained using the Total Station.

4. RESULTS OF MEASUREMENTS

Two series of measurements (Set 1, Set 3) have been available in which the position of the pipe T relative to the LRL has been chosen to be misaligned by $d \leq 0.5$ mm corresponding to the linear portion of the calibration curve and one series of measurements (Set 2) with $d \geq 0.5$ mm, which corresponds to the nonlinear portion of the curve. The comparison of the results can be found in the table.

Total Station – LRL difference Δ , mm	Set 1		Set 3		Set 2	
	Pipe end centers		Pipe end centers		Pipe end centers	
	B ₁	B ₂	B ₁	B ₂	B ₁	B ₂
Horizontal	0.06	0.02	-0.07	-0.15	0.12	0.37
Vertical	-0.13	-0.11	-0.07	-0.15	-0.41	-0.35

It is visible from the table that:

— in the Set 1 and Set 3 data the average difference is $\overline{\Delta} = -0.07$ mm with a spread of individual differences in the interval from -0.15 to 0.06 mm;

— in the Set 2 data the values are $\overline{\Delta} = 0.07$ mm with a spread of individual differences in the interval from -0.41 to 0.37 mm.

With the measurement error of the Total Station estimated to be ± 0.12 mm for this application and the error of the laser measurement estimated to be ± 0.03 mm (Fig. 16), the results of Set 1 and Set 2 agree statistically.

The larger spread of individual measurements in Set 2 relative to Set 1 and Set 3 appears to be caused by:

- the nonlinearity of the calibration curve and a misalignment $d \geq 0.5$ mm of the pipe T with respect to the laser beam;
- insufficiently accurate angular positioning of the quadrant photodetector cross-hairs in phi.

Thus, the coincidence region of the Total Station and LRL measurements has been determined from a comparison of the results got by both measurement techniques. This region is limited by the linear portion of the calibration curve for the LRL measurements $\delta \leq 0.5$ mm (Fig. 14).

To perform measurements with $d \geq 1$ mm, the LRL should be modified by:

- using the laser beam with a larger diameter at the measurement point;
- equipment of the quadrant photodetector with sensor to define the rotation phi around the laser beam axis.

CONCLUSIONS

An original method for highly accurate measurements of the alignment of beam pipe ends on a reference axis has been proposed and tested. The test measurements have been performed using jointly the LRL in a 2D local coordinate system and a Total Station survey instrument in a global 3D coordinate system. The fiducial marks at the pipe ends have been measured with both instrumentations. A transformation to a common coordinate system has been applied to allow the comparison of the results.

The results of the measurements coincide to an accuracy of approximately $\pm 100 \mu\text{m}$ in the directions perpendicular to a common reference line close to the laser beam and for a pipe place at the middle of a 50 m line.

The test shows that the proposed LRL system is a promising method for the on-line positioning and monitoring of 2D coordinates of fiducial marks. It could be used for highly precise alignment of equipment linearly distributed.

The tested system could be improved using the innovative laser-based metrological techniques [8–11] that employ the phenomena of increased stability of the laser beam position in the air when it propagates in a pipe as it works as a three-dimensional acoustic resonator with standing sound waves could be integrated in the setup. This property is the physical basis for the development of a measurement technique with a significant gain in attainable accuracy.

Acknowledgements. The authors (Dubna part) are grateful to V. Bednyakov for the significant scientific interest and vitally important financial support. At the early stage of laser metrology development, the help of C. Lasseur was substantial.

REFERENCES

1. *Batusov V. et al.* Photodetector Noise Limitations of the Laser Ray Space Localization Precision. JINR Commun. E13-2008-90. Dubna, 2008. 6 p.
2. *Batusov V. et al.* Development and Application of High-Precision Metrology for the ATLAS Tile-Calorimeter Construction (Pre-assembly Experience and Lessons). JINR Commun. E13-2004-177. Dubna, 2004. 26 p.

3. *Batusov V. et al.* High Precision Laser Control of the ATLAS Tile-Calorimeter Module Mass Production at JINR // *Part. Nucl., Lett.* 2001. No. 2 [105]. P.33–40.
4. *Batusov V. et al.* Development of Laser Measurements at the ATLAS Tile Calorimeter Module Production. JINR Commun. E13-2001-257. Dubna, 2001.
5. *Batusov V. et al.* Comparison of ATLAS Tile Calorimeter Module High Precision Metrology Measurement Results Obtained by Laser (JINR) and Photogrammetric (CERN) Methods // *Part. Nucl., Lett.* 2002. No. 4 [113]. P. 36–50.
6. *Leica A. G.* Photogrammetry and Metrology. Unterentfelden, Switzerland. User Manual for the Wild Heerbrugg T2002, TC2002 and T3000. 1996.
7. <http://www.mouser.com/ds/2/313/QP50-6-18u-TO8-9216.pdf>
8. *Batusov V. et al.* On Some New Effect of Laser Ray Propagation in Atmospheric Air // *Phys. Part. Nucl. Lett.* 2010. V. 7, No. 5. P. 359–363.
9. *Batusov V. Yu. et al.* Observation of Specific Features of Laser Beam with Propagation in Air Standing Acoustic Waves // *Ibid.* No. 1. P. 33–38.
10. *Batusov V. et al.* A Study of an Air Medium Influence on the Rectilinearity of Laser Ray Proliferation towards the Using for Large Distances and High-Precision Metrology // *Phys. Part. Nucl. Lett.* 2007. V. 4, No. 1. P. 92–95.
11. *Batusov V. et al.* Laser Beam Fiducial Line Application for Metrological Purposes // *Phys. Part. Nucl.* 2009. V. 40, No. 1. P. 115–129.

Received on September 11, 2013.